

## Melting Temperature and Wetting Angle of AlN/Dy<sub>2</sub>O<sub>3</sub> and AlN/Yb<sub>2</sub>O<sub>3</sub> Mixtures on SiC Substrates

Aline Corecha Santos<sup>a\*</sup>, Ana Paula Luz<sup>b</sup>, Sebastião Ribeiro<sup>a</sup>

<sup>a</sup>Engineering School of Lorena – EEL, Universidade de São Paulo – USP, Pólo Urbo Industrial, Gleba AI6, CP 116, CEP 12608-970, Lorena, SP, Brazil

<sup>b</sup>Materials Engineering Department, Universidade Federal de São Carlos – UFSCar, Rod. Washington Luiz, Km 235, CEP 13565-905, São Carlos, SP, Brazil

Received: April 27, 2015; Revised: September 8, 2015

This work aims to evaluate the melting temperature and wetting behavior of AlN/Re<sub>2</sub>O<sub>3</sub> (Re = Dy, Yb) mixtures when in contact with SiC substrates at high temperatures, in order to define whether these compounds can be further used to induce a more effective liquid phase sintering of SiC-based products. The prepared samples were placed on SiC plates and thermally treated up to 1900 °C under argon. The melting point and spreading evolution of different compositions of AlN/Re<sub>2</sub>O<sub>3</sub> on SiC were determined by analyzing images captured as a function of the heating temperature. The contact angle and melting point were measured using the ImageJ software and according to DIN 51730, respectively. Based on the obtained wetting curves, all evaluated conditions resulted in the decrease of the contact angle values with temperature. The mixtures presenting improved wetting ( $\theta \sim 1^\circ$  and  $3^\circ$ ) on SiC plates were the ones above the selected eutectic point.

**Keywords:** SiC, AlN, rare earth oxides, wettability, contact angle

### 1. Introduction

The sintering process of ceramics can be sped up in the presence of liquid phases, allowing a significant reduction of the temperature and time required for an effective densification of the materials microstructure<sup>1</sup>. Due to the limitations related to the solid phase sintering process of SiC-based products, the search for compounds that can induce liquid generation at high temperatures and, consequently, favor the sintering/densification transformations, is highly recommended in order to develop ceramics with better performance<sup>2</sup>. Furthermore, not only the type but also the amount of additives (used to result in the liquid phase formation) will have a major effect on the mechanical properties of the SiC obtained via liquid phase sintering (LPS).

Negita<sup>3</sup> reported that rare earth oxides (Re<sub>2</sub>O<sub>3</sub>) show greater stability when interacting with silicon carbide at high temperatures. Moreover, the blend of aluminum nitride (AlN) with these compounds is also an effective alternative to optimize the properties (i.e. fracture toughness, etc.) of such ceramic<sup>4</sup>. Based on the various investigations presented in the literature, the following systems have been evaluated for this purpose: AlN – Re<sub>2</sub>O<sub>3</sub> (Re = Y, La e Nd)<sup>[5]</sup>, AlN – Y<sub>2</sub>O<sub>3</sub><sup>[6,7]</sup>, AlN – Re<sub>2</sub>O<sub>3</sub> (Re = Y e Yb)<sup>[8]</sup>, AlN – Re<sub>2</sub>O<sub>3</sub> (Re = Y, Er e Yb)<sup>[9]</sup>, AlN – Re<sub>2</sub>O<sub>3</sub> (Re = Y, Yb, Er, Lu, Ho, Sm e Ce)<sup>[10]</sup>, AlN – Re<sub>2</sub>O<sub>3</sub> (Re = Y, Yb, La)<sup>[11]</sup>.

Considering the available phase diagrams for rare earth oxides - aluminum nitride, AlN-Y<sub>2</sub>O<sub>3</sub> system has been the most investigated one. Based on thermodynamic calculations, Kaufman et al.<sup>12</sup> predicted a diagram for this

latter system, highlighting that a simple eutectic transformation could describe the equilibrium among the various phases. Jeutter<sup>13</sup> indicated via experimental tests that the eutectic composition could be attained for compositions comprising approximately 43% mol of AlN + 57% mol of Y<sub>2</sub>O<sub>3</sub>. Aiming to understand the SiC sintering process in the presence of AlN-Re<sub>2</sub>O<sub>3</sub> for the *in situ* liquid-phase formation, the study of different parameters [i.e., interfacial energy between solid and liquid phases, surface tension, liquid penetration along grain boundaries of the solid-solid contacts (dihedral angle), wetting (contact angle), and infiltration by capillary action] are of most importance<sup>14-16</sup>.

For instance, after the liquid generation during the LPS, the resultant microstructure of the consolidated ceramics should contain solid, liquid and vapor phases. With the liquid spreading on the solid surface, the decrease of the solid-vapor interface, followed by the increase of solid-liquid and liquid-vapor ones, should take place. Figure 1 illustrates the usual liquid spreading evolution when a good or poor wetting is detected on a solid surface. Young's equation suitably describes the equilibrium condition reached for a system in the horizontal plane, where the contact angle ( $\theta$ ) is associated with the balance of three interfacial energies,  $\gamma^{SV}$ ,  $\gamma^{SL}$ , and  $\gamma^{LV}$  (Equation 1).

$$\gamma^{LV} \cos\theta = \gamma^{SV} - \gamma^{SL} \quad (1)$$

The letters S, L, and V represent solid, liquid, and vapor components, respectively. The  $\gamma^{SV} - \gamma^{SL}$  difference is the wetting driving force and the solid should be wetted when  $\gamma^{LV} \cos\theta > 0$ .

\*e-mail: alinecorecha@yahoo.com.br

The work of adhesion ( $W_a$ ) between solid and liquid can be expressed by the Dupre's equation as follows:

$$W_a = \gamma^{LV} + \gamma^{SV} - \gamma^{SL} \quad (2)$$

The combination of Equations 1 and 2 give rise to the Young-Dupre equation:

$$W_a = \gamma^{LV} (\cos\theta + 1) \quad (3)$$

and when  $\theta = 0$ ,  $\cos \theta$  will be equal to 1, resulting in the following:

$$W_a = 2\gamma^{LV} \quad (4)$$

Equation 4 shows that  $W_a$  (work of adhesion) is equivalent to twice the value of the liquid surface tension, which is related to the minimum energy required to break the liquid column per unit of area. In this case, the liquid-solid work of adhesion is equivalent or exceeds the cohesion work of the liquid, allowing this phase to spread on the solid surface.

It is accepted that: (i) for  $\theta > 90^\circ$ , the liquid will not wet the solid material, (ii) when  $\theta < 90^\circ$ , there will be the surface wetting and the liquid should spontaneously spread on it, (iii) when  $\theta \approx 0^\circ$ , the liquid should spread on the solid indefinitely, resulting in a complete wetting of the considered surface. It is important to highlight that, considering the liquid phase sintering process of ceramic materials, a suitable condition to favor the microstructure sintering is obtained when  $\theta < 90^\circ$ .

An alternative to evaluate liquid wettability consists in the measurement of the contact angle formed between the liquid and solid interface as a function of the temperature, time and liquid composition. The sessile drop technique is one of the most used experimental procedures for this purpose, as with a photographic system, images of the solid substrate + sample that will be melted (giving rise to the liquid phase when increasing the temperature) can be obtained, leading to an accurate determination of the shape evolution of the molten component. The contact angle is further calculated with an appropriate image analyzing software<sup>7,17-19</sup>.

This work was mainly focused on the wetting evaluation of SiC plates by AlN/Dy<sub>2</sub>O<sub>3</sub> and AlN/Yb<sub>2</sub>O<sub>3</sub> mixtures, as a function of temperature and time using the sessile drop method. The measurements carried out in this investigation aimed to attain a better understanding of the wetting behavior of the analyzed compositions, in order to determine the likelihood of using them as suitable options to induce an effective liquid phase sintering of SiC-based materials.

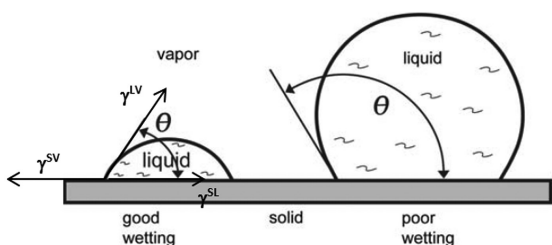


**Figure 1.** Wetting of a liquid on the horizontal plane showing low and high contact angle<sup>1</sup>.

## 2. Material and Methods

No AlN-Dy<sub>2</sub>O<sub>3</sub> and AlN-Yb<sub>2</sub>O<sub>3</sub> phase diagrams could be found in the consulted literature. However, due to the similar properties of the rare earth oxides<sup>3</sup>, it was decided to take as reference the diagram shown in Figure 2 (AlN-Y<sub>2</sub>O<sub>3</sub>) for the selection of the compositions to be analyzed in this work.

Firstly, AlN-Dy<sub>2</sub>O<sub>3</sub> and AlN-Yb<sub>2</sub>O<sub>3</sub> mixtures equivalent to the eutectic point (43.05 mol% AlN and 56.95 mol% Re<sub>2</sub>O<sub>3</sub>, dotted vertical line 3 in Figure 2) were evaluated. Moreover, additional compositions near the eutectic point but containing the increment or reduction of 5 mol% or 10 mol% of Y<sub>2</sub>O<sub>3</sub> (see dotted vertical lines in Figure 2) were also selected in order to identify which one of them would result in liquid phase generation at the lowest temperature. Table 1 presents details of the prepared AlN-Dy<sub>2</sub>O<sub>3</sub> and AlN-Yb<sub>2</sub>O<sub>3</sub> compositions.

It was used as precursor powder dysprosium oxide and ytterbium oxide with 99.9% purity supplied by ABCR GmbH & Co (< 1 μm) and aluminum nitride supplied by Hermann C. Starck Grade C (< 8 μm) - Germany. The raw materials were weighed on a precision scale (± 0.01 grams) according to the amounts defined in Table 1. After that, they were mixed in a planetary mill for 20 minutes (using isopropyl alcohol as liquid medium), dried at 110 °C for 24 hours and pressed into a cylindrical die with 4 mm diameter and 3 mm length.

For the wetting measurements, the pressed samples were placed on the top surface of prepared SiC plates (which had 98.9% of density). The set (pressed sample + SiC plate) was initially introduced in a graphite resistance furnace (ASTRO) and heated at a rate of 24 °C/min up to 1000 °C or 1800 °C for AlN/Dy<sub>2</sub>O<sub>3</sub> or AlN/Yb<sub>2</sub>O<sub>3</sub> compositions, respectively. After reaching this temperature, a lower heating rate was used (5 °C/min) under argon atmosphere at 1 atm, in order to define the materials' melting point and analyze the spreading behavior of the liquid. The time effect on the wetting evolution of the prepared SiC substrates was analyzed with the use of one sample of each system (AlN-Dy<sub>2</sub>O<sub>3</sub> e AlN-Yb<sub>2</sub>O<sub>3</sub>), equivalent to the composition that presented the lower contact angle values. Therefore, after reaching the melting point of these mixtures, it was carried out a holding step at this temperature (by changing the power provided

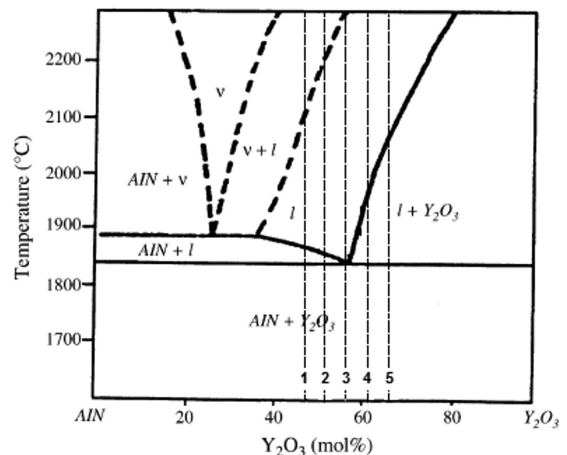


**Figure 2.** AlN-Y<sub>2</sub>O<sub>3</sub> phase diagram obtained by Jeutter<sup>13</sup>.

to the Astro furnace in order to keep the temperature at a constant value) to determine the time required to result in a complete wetting of the solid surface (equilibrium condition).

The changes in the shape of the AlN-Dy<sub>2</sub>O<sub>3</sub> e AlN-Yb<sub>2</sub>O<sub>3</sub> pressed samples on the SiC plate with temperature and time was observed by using an image capture system (Figure 3) to obtain the maximum liquid spreading. The contact angle values were determined with the analysis of the captured images

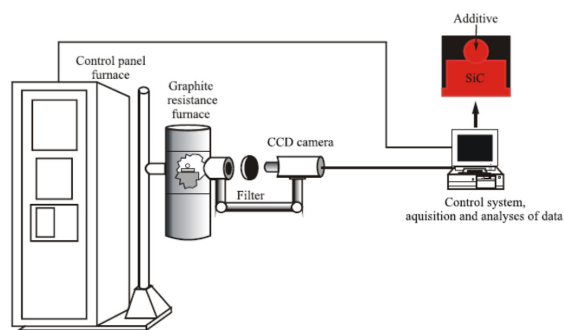


Figure 3. Scheme of the wettability testing system<sup>17</sup>.

using the ImageJ software (version 1.45s). Furthermore, the melting temperature of the AlN/Dy<sub>2</sub>O<sub>3</sub> e AlN/Yb<sub>2</sub>O<sub>3</sub> mixtures was calculated according to the procedure described in the DIN 51730 standard<sup>20</sup>.

After the furnace's cooling down, the collected samples were cut and had their cross-section area ground, polished and coated with gold for the microstructural analysis. The liquid phase + SiC contact interface was analyzed via scanning electron microscope (SEM, LEO, model 1450VP) with energy dispersive spectrometer (EDS, Oxford INCA system).

### 3. Results and Discussion

Figure 4 shows the representative behavior of AlN/Dy<sub>2</sub>O<sub>3</sub> and AlN/Yb<sub>2</sub>O<sub>3</sub> mixtures on SiC plates with the increase of the temperature. Figure 4a and 4d indicate the condition where the pressed cylinders still presented their original shape, as the furnace's temperatures were below the respective melting points of the evaluated materials. With the temperature increase, these samples changed their shape and the formation of a half-sphere (Figure 4b and 4e) represented the melting point of the mixtures, according to DIN51730 standard.

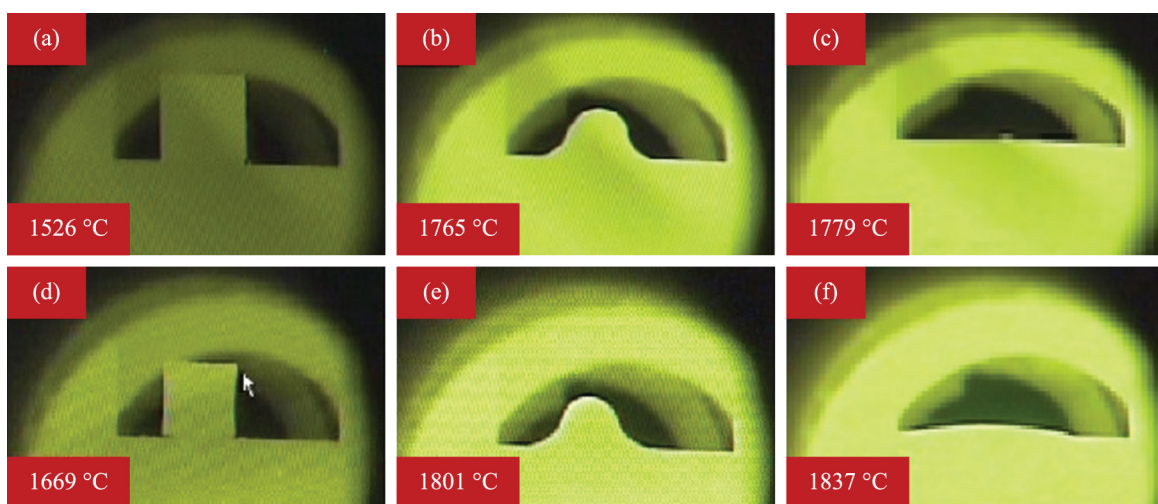


Figure 4. Sequence of images obtained via CCD camera during the wetting measurements of AlN/Dy<sub>2</sub>O<sub>3</sub> (a-c) and AlN/Yb<sub>2</sub>O<sub>3</sub> representative mixtures (d-f) on SiC substrates.

Table 1. Composition of the AlN-Re<sub>2</sub>O<sub>3</sub> mixtures evaluated in this work.

Code* <sup>1</sup>	mol %			weight %			Notes* <sup>2</sup>
	AlN	Dy <sub>2</sub> O <sub>3</sub>	Yb <sub>2</sub> O <sub>3</sub>	AlN	Dy <sub>2</sub> O <sub>3</sub>	Yb <sub>2</sub> O <sub>3</sub>	
1D	53.05	46.95	-	11.04	88.96	-	10% B
2D	48.05	51.95	-	9.22	90.78	-	5% B
3D	43.05	56.95	-	7.67	92.33	-	supposed eutectic
4D	38.05	61.95	-	6.32	93.68	-	5% A
5D	33.05	66.95	-	5.14	94.86	-	10% A
1Y	53.05	-	46.95	10.52	-	89.48	10% B
2Y	48.05	-	51.95	8.77	-	91.23	5% B
3Y	43.05	-	56.95	7.29	-	92.71	supposed eutectic
4Y	38.05	-	61.95	6	-	94	5% A
5Y	33.05	-	66.95	4.88	-	95.12	10% A

\*<sup>1</sup> D and Y indicate "dysprosium" and "ytterbium", respectively. \*<sup>2</sup> A and B indicate "after" and "before" the eutectic composition, respectively.

**Table 2.** Melting temperature (MT), final (CA<sub>f</sub>) and initial (CA<sub>i</sub>) contact angle of the evaluated compositions.

Mixtures	AlN-Dy <sub>2</sub> O <sub>3</sub>					AlN-Yb <sub>2</sub> O <sub>3</sub>					
	code	1D	2D	3D	4D	5D	1Y	2Y	3Y	4Y	5Y
MT (°C)		1767	1765	1760	1765	1761	1818	1801	1820	1813	1827
CA <sub>i</sub> (°)		51	50	32	51	36	46	48	42	52	46
CA <sub>f</sub> (°)		5	3	4	1	7	9	7	4	6	3

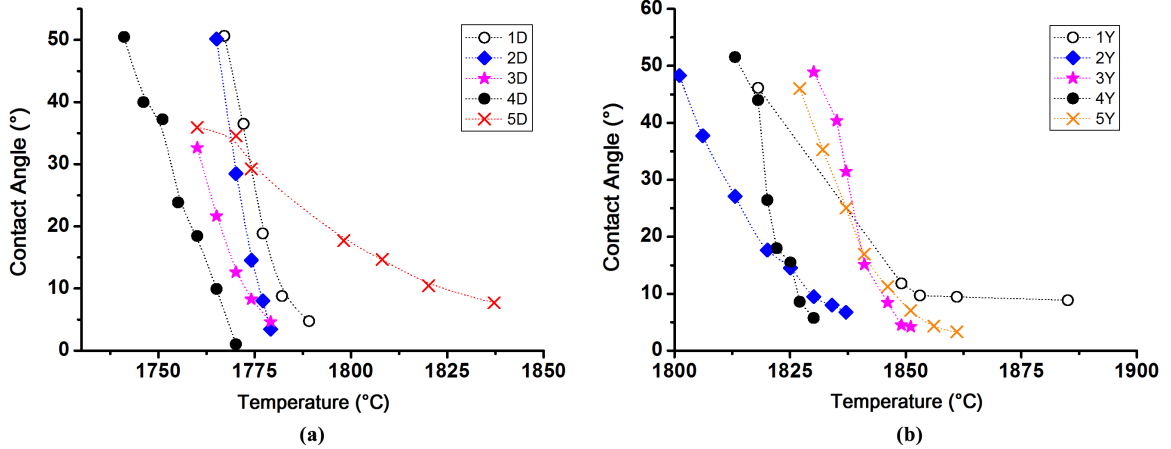


**Figure 5.** Temperature influence on the contact angle of (a) AlN/Dy<sub>2</sub>O<sub>3</sub> and (b) AlN/Yb<sub>2</sub>O<sub>3</sub> mixtures on SiC substrates.

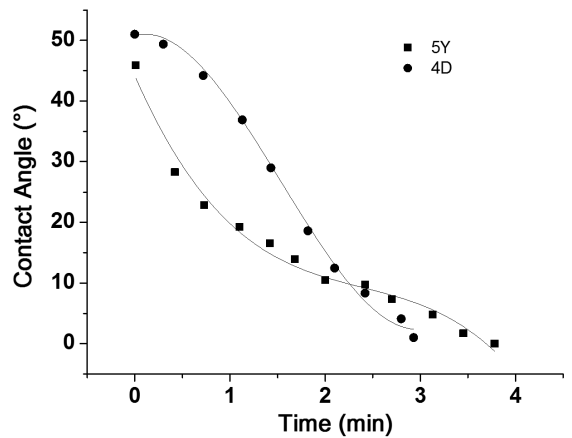
Furthermore, Figure 4c and 4f also indicate the complete spreading of the liquid phase on the SiC plates.

Figure 5 shows the contact angle evolution with temperature and, a general trend observed was the decrease of  $\theta$  with the increase of the temperature. This behavior was associated to the reduction of the solid/liquid interfacial energy, that according Equation 1, favoring the liquid spreading at high temperature. Compositions 4D and 5Y presented the smallest contact angles, indicating the better wetting and spreading of the liquid phases. Moreover, all evaluated compositions exhibited very good wettability ( $\theta \ll 90^\circ$ ) with final contact angles smaller than  $10^\circ$ . Such results are in tune with the data related to compositions of the AlN/Y<sub>2</sub>O<sub>3</sub> system (measured contact angle  $\sim 6^\circ$  at  $1870^\circ\text{C}$ )<sup>7</sup>.

Table 2 shows the melting temperature (MT), initial contact angle (CA<sub>i</sub>) obtained at the melting temperature where formation of the liquid was observed (samples' shape = half-sphere) and final contact angle (CA<sub>f</sub>) measured after the complete liquid spreading.

The melting temperatures of the studied compositions and the deviation of these values were equivalent to  $\pm 15^\circ\text{C}$  (depending on the moment when the images were captured). It is important to highlight that the sessile drop technique and the contact angle measurements are easy to be implemented, but one should take care in the selection of the images related to the half-sphere formation, as determined by the DIN 51730 standard.

In general, dysprosium oxide-containing compositions melted at lower temperatures than the ones with ytterbium oxide. However, the evaluated mixtures presented similar results, pointing out that the two studied systems must have a eutectic transformation as shown in Figure 2.



**Figure 6.** Contact angle ( $\theta$ ) versus time (t) for the 4D and 5Y mixtures on SiC substrates.

Figure 6 illustrates the contact angle behavior versus time for the mixtures that presented the lowest  $\theta$  values (4D and 5Y) considering isothermal conditions and keeping the samples at the temperatures indicated in Table 2. Based on these tests, the maximum spreading (complete wetting of the SiC surface) was obtained after approximately 3 and 4 minutes for the 4D and 5Y samples, respectively. The  $\theta$  decay for 4D mixture was initially faster than for 5Y and this behavior might be associated to viscosity of the formed liquid, as this property is one of the main factors influencing the liquid spreading speed and considering that the quality of the surfaces of the SiC plates were the same.



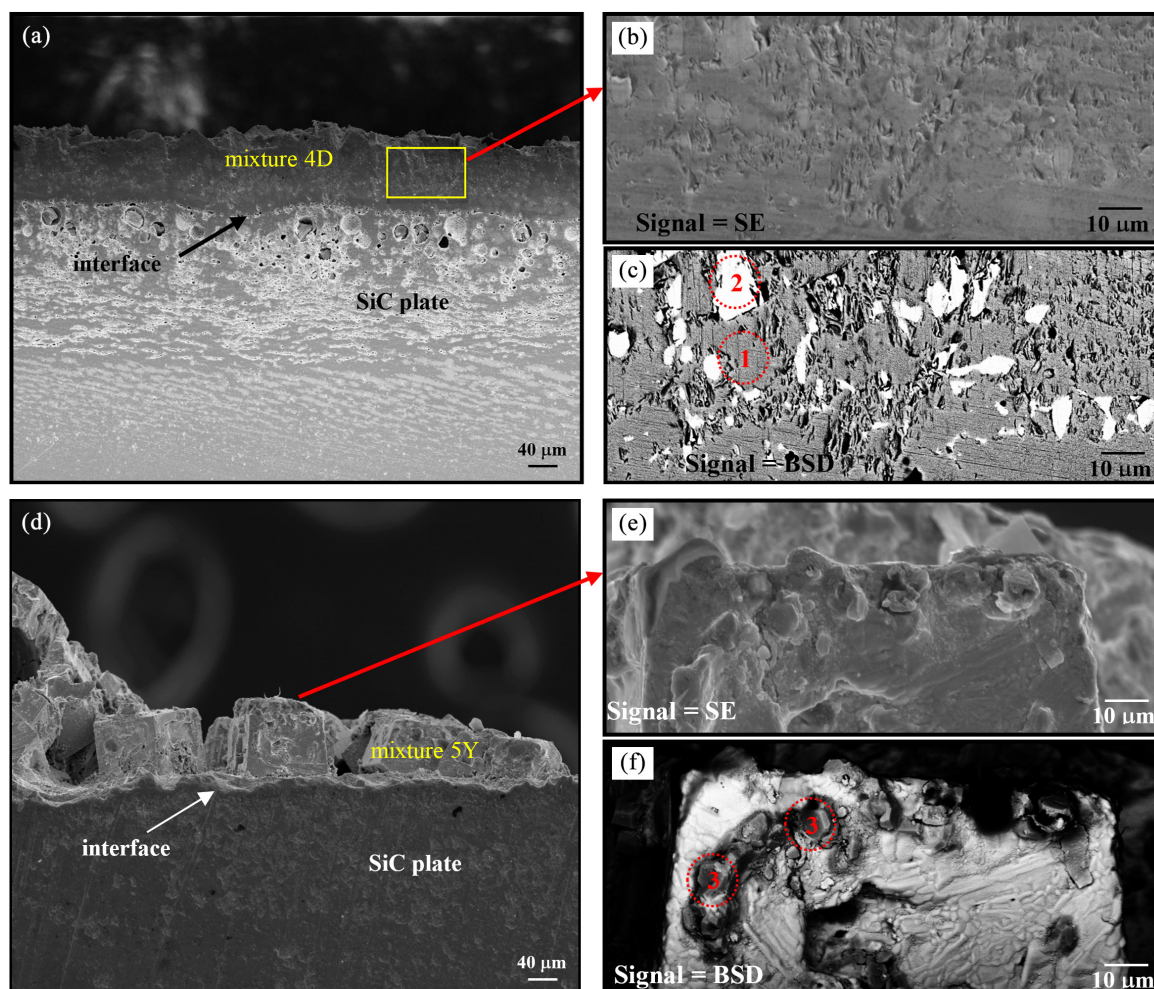


**Figure 7.** SEM images of the interface area between SiC + 4D (a) and 5Y (d) compositions. Higher magnification of the regions corresponding to the liquid phase generated at high temperatures obtained via secondary electrons (b, e) and backscattered electrons emission (c, f).

Figure 7a and 7d present the images of the interface area of SiC plate + 4D or 5Y compositions. The Dy<sub>2</sub>O<sub>3</sub>-AlN-based sample showed a uniform spreading on the solid surface with the generation of a continuous and dense layer of the resultant material. On the other hand, the analysis of the liquid-solid contact area for the mixture containing Yb<sub>2</sub>O<sub>3</sub>-AlN confirmed that a non-homogeneous layer presenting regions with high or low thickness was generated after exposing this material to 1850 °C.

According to semi-quantitative EDS analyses of the SiC substrate, Dy and Yb elements could be identified in the area near the solid-liquid interface, and this latter compound was found in greater content (Dy: 8.96 wt% or Yb: 65.95 wt%), which suggests that liquid infiltration might have taken place into the SiC plate microstructure.

Further details of the samples' microstructure can be observed in Figure 7b-e (secondary electrons mode) and 7c-f (backscattered electrons). EDS analyses of the region presented in Figure 7c indicated that the darkest region (1) is comprised by C - Al - Si, suggesting that a partial dissolution of SiC took place into the liquid phase at high temperature, and the lighter area (2) is rich in Dy. The magnified region

exhibited in Figure 7f (3) points out the presence of very small hexagonal crystals containing C - N - Al, also indicating the silicon carbide dissolution into the liquid and possibly a further precipitation of AlN.

#### 4. Conclusions

According to the obtained results, the wettability of SiC surface depends strongly on the temperature, as the resultant contact angle of the molten AlN/Re<sub>2</sub>O<sub>3</sub> compositions presented a major decrease at higher temperatures, leading to the liquid spreading on the solid plates. The evaluated rare earth oxides (Dy<sub>2</sub>O<sub>3</sub> and Yb<sub>2</sub>O<sub>3</sub>) showed similar wetting behavior on the silicon carbide substrates. AlN/Dy<sub>2</sub>O<sub>3</sub> and AlN/Yb<sub>2</sub>O<sub>3</sub> mixtures presented final contact angles smaller than 10°, which can allow their use as efficient additives for the liquid phase sintering of SiC-based ceramics.

The compositions of rare earth oxides above the supposed eutectic point (AlN 43.05% - 56.95 mol% Re<sub>2</sub>O<sub>3</sub>) resulted in liquid infiltration in the SiC plate. The liquid spreading behavior as a function of time (isothermal condition) indicated that the AlN/Dy<sub>2</sub>O<sub>3</sub> composition presented a more significant

drop, most likely due to the formation of a larger volume fraction of liquid in the melting temperature. Carbon was detected at the SiC - AlN/Re<sub>2</sub>O<sub>3</sub> interface and also inside the layer derived from the liquid phase formation, suggesting that a partial dissolution of SiC. Considering the difficulties commonly found in the production of dense SiC ceramics, the use of AlN-Dy<sub>2</sub>O<sub>3</sub> and AlN-Yb<sub>2</sub>O<sub>3</sub> mixtures, especially 4D and 5Y which had lower contact angle (1° and 3°) and good spreading time after the samples' melting (3 and 4 minutes), can be a suitable alternative to induce an improved sintering of this carbide compound, as the formation of the liquid (derived from the addition of these AlN/Re<sub>2</sub>O<sub>3</sub> and which

is the main driving force for the LPS) should result in a fast spreading (as observed in the contact angle measurements) and scattering of this phase in the microstructure at high temperature, leading to a more effective densification process.

## Acknowledgements

This work was supported by Fundação de Amparo à Pesquisa do Estado de São Paulo – FAPESP (Project No. 201051925-6), Conselho Nacional de Desenvolvimento Científico e Tecnológico – CNPq (Productivity grant No. 304760/2010-2), and Coordenação de Aperfeiçoamento de Pessoal de Nível Superior – CAPES.

## References

1. Randall GM. *Sintering theory and practice*. New York: John Wiley & Sons; 1996.
2. Strecker K, Ribeiro S and Hoffmann MJ. Fracture toughness measurements of LPS-SiC: a comparison of the indentation technique and the SEVNB method. *Materials Research*. 2005; 8(2):121-124. <http://dx.doi.org/10.1590/S1516-14392005000200004>.
3. Negita K. Effective sintering aids for silicon carbide ceramics: reactivities of silicon carbide with various additives. *Journal of the European Ceramic Society*. 1986; 69(12):308-310. <http://dx.doi.org/10.1111/j.1151-2916.1986.tb07398.x>.
4. Kim Y-W, Chun Y-S, Nishimura T, Mitomo M and Lee Y-H. High-temperature strength of silicon carbide ceramics sintered with rare-earth oxide and aluminum nitride. *Acta Materialia*. 2007; 55(2):727-736. <http://dx.doi.org/10.1016/j.actamat.2006.08.059>.
5. Wu L, Chen Y, Jiang Y and Huang Z. Liquid phase sintering of SiC with AlN-Re<sub>2</sub>O<sub>3</sub> additives. *Journal of the Chinese Ceramic Society*. 2008; 36(5):593-596.
6. Ye H, Rixecker G, Haug S and Aldinger F. Compositional identification of the intergranular phase in liquid phase sintered SiC. *Journal of the European Ceramic Society*. 2002; 22(13):2379-2387. [http://dx.doi.org/10.1016/S0955-2219\(02\)00006-7](http://dx.doi.org/10.1016/S0955-2219(02)00006-7).
7. Balestra RM, Ribeiro S, Taguchi SP, Motta FV and Bormio-Nunes C. Wetting behaviour of Y<sub>2</sub>O<sub>3</sub>/AlN additive on SiC ceramics. *Journal of the European Ceramic Society*. 2006; 26(16):3881-3886. <http://dx.doi.org/10.1016/j.jeurceramsoc.2005.12.022>.
8. Kim Y-W, Mitomo M and Nishimura T. High-temperature strength of liquid-phase-sintered SiC with AlN and Re<sub>2</sub>O<sub>3</sub> (RE = Y, Yb). *Journal of the American Ceramic Society*. 2002; 85(4):1007-1009. <http://dx.doi.org/10.1111/j.1151-2916.2002.tb00211.x>.
9. Choi H-J, Lee J-G and Kim Y-W. Oxidation behavior of liquid-phase sintered silicon carbide with aluminum nitride and rare-earth oxides (Re<sub>2</sub>O<sub>3</sub>, where Re = Y, Er, Yb). *Journal of the American Ceramic Society*. 2002; 85(9):2281-2286. <http://dx.doi.org/10.1111/j.1151-2916.2002.tb00448.x>.
10. Magnani G, Antolini F, Beaulardi L, Burrelli E, Coglitore A and Mingazzini C. Sintering, high temperature strength and oxidation resistance of liquid-phase-pressureless-sintered SiC-AlN ceramics with addition of rare-earth oxides. *Journal of the European Ceramic Society*. 2009; 29(11):2411-2417. <http://dx.doi.org/10.1016/j.jeurceramsoc.2008.12.020>.
11. Izhevskiy VA, Genova LA, Bressiani JC and Bressiani AHA. Liquid phase sintered SiC: processing and transformation controlled microstructure tailoring. *Materials Research*. 2000; 3(4):131-138. <http://dx.doi.org/10.1590/S1516-1439200000400007>.
12. Kaufman L, Hayes F and Birnie D. Calculation of quasibinary and quasiternary oxyntiride systems-IV. *Calphad*. 1981; 5(3):163-184. [http://dx.doi.org/10.1016/0364-5916\(81\)90019-5](http://dx.doi.org/10.1016/0364-5916(81)90019-5).
13. Jeutter A. *Untersuchung der Phasenbeziehungen im System Aluminiumnitrid-Yttriumoxid*. [Thesis]. Germany: University of Stuttgart; 1993.
14. Kingery WD. *Ceramic fabrication process*. New York: John Wiley & Sons; 1958. p. 131-146.
15. Taguchi SP, Ribeiro S and Balestra RM. Infiltration of Al<sub>2</sub>O<sub>3</sub>/Y<sub>2</sub>O<sub>3</sub> mix into SiC ceramic preforms. *Ceramics International*. 2008; 34(3):625-629. <http://dx.doi.org/10.1016/j.ceramint.2007.01.001>.
16. Bighetti CMM, Ribeiro S, Borges SPT, Strecker K, Machado JPB and Santos C. Characterization of rare earth oxide-rich glass applied to the glass-infiltration of a ceramic system. *Ceramics International*. 2014; 40(1):1619-1625. <http://dx.doi.org/10.1016/j.ceramint.2013.07.052>.
17. Motta FV, Balestra RM, Ribeiro S and Taguchi SP. Wetting behaviour of SiC ceramics. *Materials Letters*. 2004; 58(22-23):2805-2809. <http://dx.doi.org/10.1016/j.matlet.2004.05.005>.
18. Taguchi SP, Motta FV, Balestra RM and Ribeiro S. Wetting behaviour of SiC ceramics. *Materials Letters*. 2004; 58(22-23):2810-2814. <http://dx.doi.org/10.1016/j.matlet.2004.05.004>.
19. Ribeiro S, Taguchi SP, Motta FV and Balestra RM. The wettability of SiC ceramics by molten E<sub>2</sub>O<sub>3</sub>(ss)/AlN (E<sub>2</sub>O<sub>3</sub>(ss)=solid solution of rare earth oxides). *Ceramics International*. 2007; 33(4):527-530. <http://dx.doi.org/10.1016/j.ceramint.2005.10.026>.
20. Deutsches Institut für Normung - DIN. *DIN 51730: determination of fusibility of fuel ash*. Germany; 1984.